The Lemaître-Tolman and Szekeres models and some of their applications in cosmology

Andrzej Krasiński

Work done in collaboration with Charles Hellaby (Cape Town)
and Krzysztof Bolejko (Sydney)

Contents

1 Geometry of the cosmological models

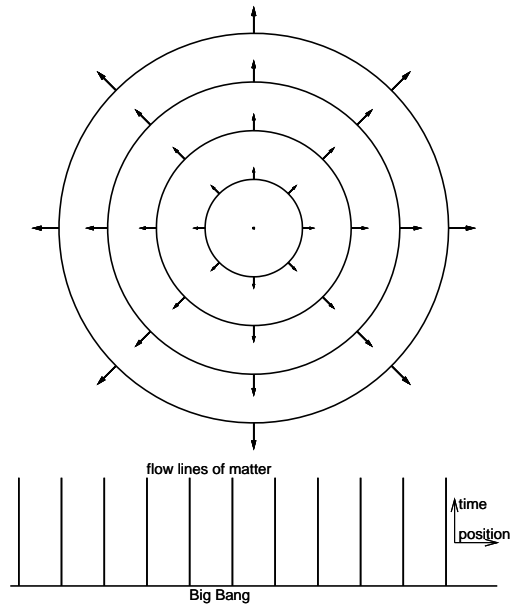## The Robertson – Walker (R–W) models

Figure 1: Expansion in the R–W models. **Upper picture:** The *velocity of expansion* of each matter shell *is proportional to its distance from the observer*. **Lower picture:** The *Big Bang occurs simultaneously* in the coordinates of (1.1).

The metric of this model is

$$ds^2 = dt^2 - S^2(t) \left[\frac{dr^2}{1 - kr^2} + r^2 \left(d\vartheta^2 + \sin^2 \vartheta d\varphi^2 \right) \right]. \qquad (1.1)$$

If pressure is zero, then $S(t)$ obeys

$$S_{,t}^2 = 2GM/(c^2 S) - k + \Lambda S^2/3, \qquad (1.2)$$

where k and M are arbitrary constants and Λ is the cosmological constant.

The mass density is constant throughout space and changes only with time.
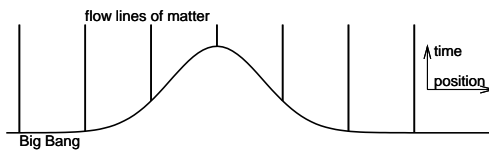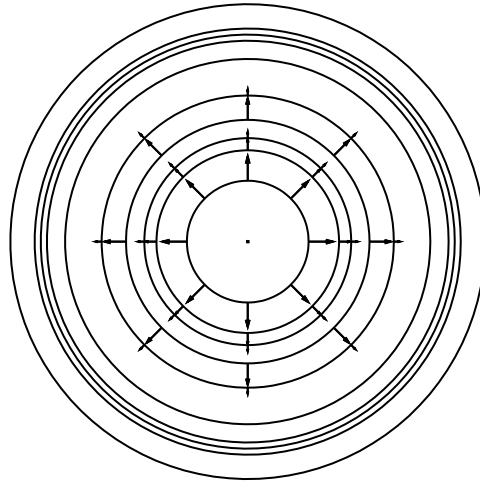
The Lemaître – Tolman (L–T) model

Figure 2: Expansion in the L–T model. **Upper picture:** The *velocity of expansion is not correlated with the radius of a matter shell*. **Lower picture:** The *Big Bang is*, in the coordinates of (1.3), *non-simultaneous* $\Longrightarrow$ the age of matter particles depends on r.

The metric of the Lemaître – Tolman [1, 2] model is

$$ds^2 = dt^2 - \frac{R_{,r}{}^2}{1 + 2E(r)} dr^2 - R^2(t,r) \left(d\vartheta^2 + \sin^2\vartheta d\varphi^2\right), \quad (1.3)$$

where $R(t,r)$ obeys (from the Einstein equations with $p = 0$):

$$R_{,t}{}^2 = 2E(r) + 2M(r)/R - \Lambda R^2/3. \quad (1.4)$$

$M(r)$ and $E(r)$ are arbitrary functions. The integral of (1.4) contains one more arbitrary function, $t_B(r)$ – the "timetable" of the Big Bang. For example, when $E = 0 = \Lambda$:

$$R = (9M/2)^{1/3} (t - t_B(r))^{2/3}. \quad (1.5)$$

The R–W limit of L–T is

$$M = \text{const} \times r^3, \quad E = -kr^2/2, \quad t_B = \text{const},$$
$$R = rS(t). \quad (1.6)$$
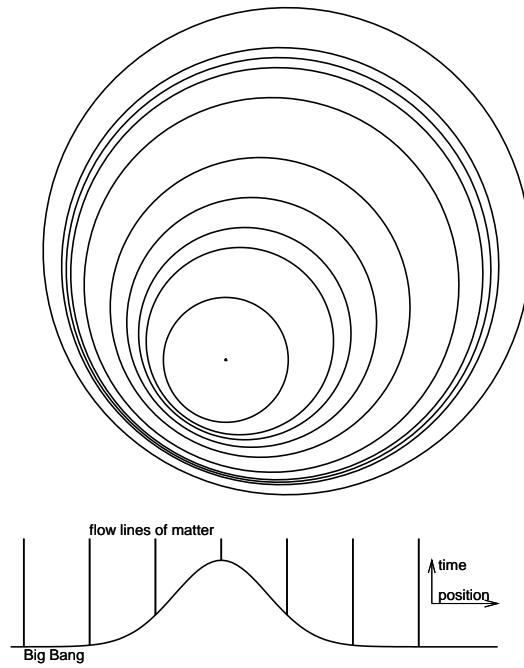
The Szekeres models

Figure 3: Expansion in the Szekeres models. **Upper picture:** The velocity of expansion is not correlated with the radius of a matter shell and *the shells are not concentric*. **Lower picture:** The "timetable" of the initial explosion looks the same as in the L–T model.

$$R_{,t}^2 = 2E(r) + 2M(r)/R - \Lambda R^2/3. \tag{1.4}$$

The metric form of the Szekeres models is [3]:

$$ds^2 = dt^2 - \frac{(R_{,r} - R\mathcal{E}_{,r}/\mathcal{E})^2}{1 + 2E(r)}dr^2 - \frac{R^2}{\mathcal{E}^2}\left(dx^2 + dy^2\right), \tag{1.7}$$

where

$$\mathcal{E} \stackrel{\text{def}}{=} \frac{S(r)}{2}\left[\left(\frac{x - P(r)}{S(r)}\right)^2 + \left(\frac{y - Q(r)}{S(r)}\right)^2 + 1\right]; \tag{1.8}$$

the function $R(t, r)$ obeys the same evolution equation (1.4) as in the L–T model; the $P(r), Q(r)$ and $S(r))$ are arbitrary functions.

The Szekeres model has in general **_no symmetry_**. It reproduces the L–T model in the limit of (P, Q, S) being constant.

The mass distribution in the Szekeres models can be interpreted as a superposition of a mass-monopole and a mass-dipole.

Please note:

The L–T and Szekeres models are not meant to be replacements for the Robertson – Walker models.

They are meant to model ***perturbations*** on the R–W background within the exact theory.

2 Formation and evolution of structures

The usual method to check a theory against observation is:

● Assume initial conditions for a physical system at $t = t_1$;

● Use the evolution equations to calculate the state of the system at $t_2 > t_1$;

● Compare the calculated result with the measurements at t_2;

● If the calculations and measurements do not agree, change the initial conditions to try a more precise "shot".

The L–T and Szekeres models allow one to use input from both t_1 and t_2 to construct a model that evolves a given state at t_1 into a given state at t_2. Examples:

Data at t_1	Data at t_2
density distribution	density distribution
velocity distribution	density distribution
velocity distribution	velocity distribution

$$R_{,t}{}^2 = 2E(r) + 2M(r)/R. \tag{1.4}$$

We will demonstrate the working of this method for the **density** $\rightarrow$ **density** evolution [4] $-$ [6].

We take the solution of (1.4) in the form

$$t - t_B(r) = \int \frac{\mathrm{d}R}{\sqrt{2E + 2M/R}} \tag{2.1}$$

(see next page). In this example, we consider $E > 0$ only.

The mass-density at any instant t_0 can be converted (numerically) to $R(t_0, r)$, with $M(r)$ being used as the radial coordinate:

$$\kappa\rho = \frac{2M_{,r}}{R^2 R_{,r}} \equiv \frac{6}{(R^3)_{,M}}$$

$$\Longleftrightarrow R^3 = \int_0^M \frac{6}{\kappa\rho(\widetilde{M})} \, \mathrm{d}\widetilde{M}. \tag{2.2}$$

$$R_{,t}{}^2 = 2E(r) + 2M(r)/R. \tag{1.4}$$

The solutions of (1.4) at $t = t_i$, $i = 1, 2$ are

$$t_B = t_i - \frac{M}{(2E)^{3/2}} \left[\sqrt{(1 + 2ER_i/M)^2 - 1} - \mathrm{arcosh}(1 + 2ER_i/M) \right],$$
$$\tag{2.3}$$

where $R_i \overset{\text{def}}{=} R(t_i, M)$.

We subtract (2.3) at $t = t_1$ from (2.3) at $t = t_2$ and obtain

$$\begin{aligned} & \sqrt{(1 + 2ER_2/M)^2 - 1} - \mathrm{arcosh}(1 + 2ER_2/M) \\ & - \sqrt{(1 + 2ER_1/M)^2 - 1} + \mathrm{arcosh}(1 + 2ER_1/M) \\ & = \frac{(2E)^{3/2}}{M}(t_2 - t_1). \end{aligned} \tag{2.4}$$

Eq. (2.4) defines the function $E(M, t_1, t_2, R_1, R_2)$.

Substituting it in (2.3) we find $t_B(M, t_1, t_2, R_1, R_2)$.

E and t_B define the L–T model that evolves $R(t_1, r)$ into $R(t_2, r)$.

11

$$\sqrt{(1 + 2ER_2/M)^2 - 1} - \text{arcosh}(1 + 2ER_2/M)$$
$$-\sqrt{(1 + 2ER_1/M)^2 - 1} + \text{arcosh}(1 + 2ER_1/M)$$
$$= \frac{(2E)^{3/2}}{M}\,(t_2 - t_1)\,. \tag{2.4}$$

The solution of (2.4) with $E > 0$ exists provided $t_2 - t_1$ is sufficiently small. The solution is then unique.

When $t_2 - t_1$ is too large, then the same two states can be connected by an L–T evolution with $E < 0$.

This approach was applied to the formation of presently existing structures out of small density or velocity perturbations of a homogeneous background existing at last scattering [4, 5, 6].

The best consistency with observations was achieved for galaxy clusters. As a representative we chose the A199 cluster, for which the "Universal Density Profile" is available.

The initial mass was assumed to be $0.01 \times$ the present mass.

The initial density amplitude $\Delta\rho/\rho = 10^{-5}$ and velocity amplitude $\Delta v/v = 10^{-4}$ were within the limits set by the CMB observations.

Velocity perturbations are 10^2 times more efficient in generating structures than density perturbations. This runs counter to the common wisdom in astronomy.

When density and velocity perturbations are simultaneously present, ***a profile reversal can occur***: a void can evolve into a condensation, and vice versa.

3 Drift of light rays induced by nonsymmetric expansion

Consider two light rays in the Szekeres spacetime, the second one emitted by the same source later by τ, both arriving at the same observer. The trajectory of the first ray is

$$(t, x, y) = (T(r), X(r), Y(r)), \tag{3.5}$$

the corresponding equation for the second ray is

$$(t, x, y) = (T(r) + \tau(r), X(r) + \zeta(r), Y(r) + \psi(r)). \tag{3.6}$$

$\Longrightarrow$ The second ray intersects a given hypersurface $r = r_0$ not only later, but, in general, at a different comoving location.

$\Longrightarrow$ **In general, the two rays will intersect different sequences of intermediate matter worldlines.**

The same is true for nonradial rays in the L–T model.

$\implies$ The second ray is emitted in a different direction and is received from a different direction by the observer.

$\implies$ An observer in a general Szekeres spacetime should see each light source slowly ***drift across the sky*** [8].

The absence of this drift is a property of exceptional directions, for example of radial directions in an L–T model. In a general Szekeres spacetime such directions do not exist.

The only spacetimes in the Szekeres family in which there is no drift for all null geodesics are the Friedmann models.

$\implies$ ***Observational detection of the drift would be evidence of inhomogeneity of the Universe on large scales.***

With the technology now being developed, measurements of the drift rate will be possible (see the numerical example below).
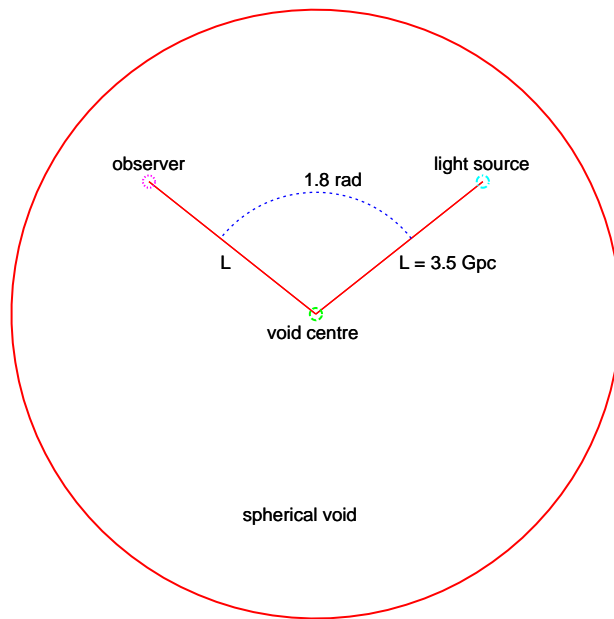
4 A numerical example of the drift

Figure 4: The L–T configuration used in the example. The present distance from the centre of the void to the observer and to the light source is $L = 3.5$ Gpc.
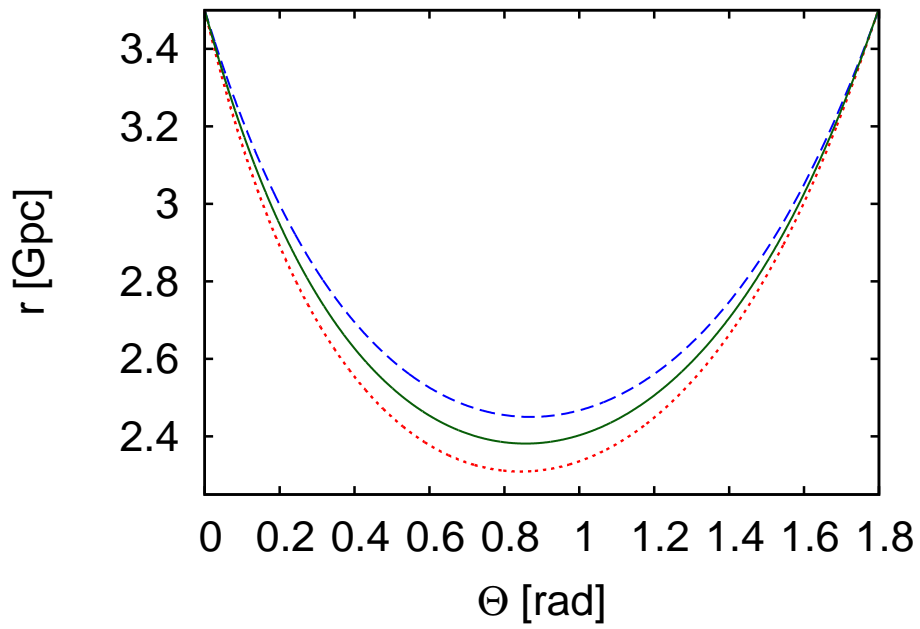
Figure 5: Rays projected on the space $t = $ now along the dust flow lines.

Middle line: ray received now.
Upper line: ray received 5×10^9 years ago.
Lower line: ray received 5×10^9 years in the future.

The rate of change of the ray direction under the most favourable conditions would be 1.5×10^{-6} **arcsec/year**.

With the Gaia accuracy[1] of $5 - 20 \times 10^{-6}$ **arc sec**, a few years would be needed to detect this effect.

---

[1] http://sci.esa.int/science-e/www/area/index.cfm?fareaid=26

5 Explaining "accelerated expansion" of the Universe by inhomogeneous mass density

The hypothesis of accelerated expansion of the Universe arose from observations of type Ia supernovae. Their maximal absolute luminosity is assumed to be the same for all.

The observed luminosities were inconsistent with the $\Lambda = 0$ Friedmann model. ***Using other Friedmann models***, the best fit to the observed luminosities was achieved when [11]

- $k = 0$,

- 32% of the energy density comes from matter (visible or dark)

- 68% of the energy density is provided by an entity that was termed "dark energy". It plays the role of the cosmological constant, but may depend on time (in an unknown way).

↑ Corrected numerical data taken from the later measurements by the Planck satellite (2013, [11]).

$\implies$ ***The "accelerated expansion" of the Universe is not an observed phenomenon, but an element of interpretation of observations. It follows from the assumption that the model must be in the Friedmann class.***

If we can re-create the observed luminosity vs. redshift relation in a decelerating inhomogeneous model, then the "accelerated expansion" becomes an illusion.

The two examples presented below [12, 13, 14, 15] show how the spurious accelerated expansion is reproduced using just one of the two arbitrary functions of the L–T model.

Example 1: $E/r^2 = $ const is the same as in the R–W models. The $t_B(r)$ is defined so that the $D_L(z)$ relation of the ΛCDM model

$$D_L(z) = \frac{1+z}{H_0} \int_0^z \frac{\mathrm{d}z'}{\sqrt{\Omega_m(1+z')^3 + \Omega_\Lambda}}, \qquad (5.1)$$

is reproduced, with $\Omega_m = 0.32$ and $\Omega_\Lambda = 0.68$; H_0 is the present value of the Hubble coefficient.

The trick is that H_0, Ω_m and Ω_Λ are taken from observations, but $D_L(z)$ is taken from an L–T model with $\Lambda = 0$, and this defines $t_B(r)$. Equations for $t_B(r)$ are then solved numerically.
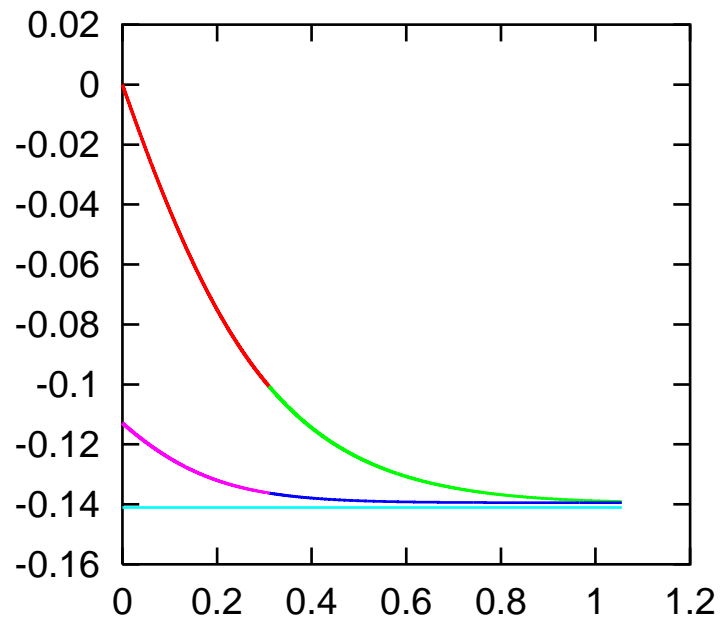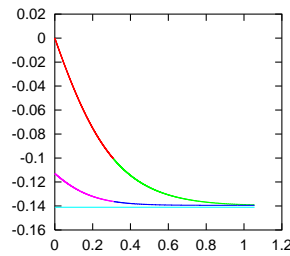
Figure 6: Example 1: The past light cone of the central observer in the L–T model that duplicates the $D_L(z)$ relation using only $t_B(r)$. The lower curve is the numerically calculated $t_B(r)$, the horizontal straight line marks the Big Bang of the ΛCDM model.

In the L–T model the Big Bang occurs progressively later when the position of the observer is approached.

$\Longrightarrow$ The time between the Big Bang and the instant of crossing the observer's past light cone becomes progressively shorter in L–T than in R–W.

$\Longrightarrow$ The expansion velocity at the light cone in the L–T model is everywhere greater than in a Friedmann model with $\Lambda = 0 = k$, and the difference is increasing toward the observer.

$\Longrightarrow$ Instead of increasing with time, the expansion velocity increases with position in space.

$\Longrightarrow$ *Had we used the L–T model to interpret the observations, the "accelerated expansion" would not be implied, and there would be no need for "dark energy".*

23

Example 2: $t_B(r)$ is constant, as in an R–W model. The equation

$$D_L(z) = \frac{1 + z}{H_0} \int_0^z \frac{dz'}{\sqrt{\Omega_m(1 + z')^3 + \Omega_\Lambda}}, \qquad (5.1)$$

is this time used to define the L–T function $E(r)$.

In this case, the graph of the light cone and of the Big Bang does not look different from the Friedmann case; the difference is in the shape of E/r^2, which is constant in Friedmann.

Recall the L–T metric:

$$ds^2 = dt^2 - \frac{R_{,r}^2}{1 + 2E(r)}dr^2 - R^2(t, r)\left(d\vartheta^2 + \sin^2\vartheta d\varphi^2\right), \quad (1.3)$$

The Friedmann limit of it is $2E = -kr^2$ and $R(t, r) = rS(t)$.

$\Longrightarrow$ **With non-constant E/r², each L–T matter shell evolves by a different Friedmann equation.**
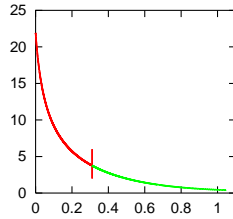
Figure 7: The function $E/r^2 = -k_F$ in Example 2. The observer is at $r = 0$, the past light cone of the observer touches the Big Bang at $r \approx 1.1$.

$E/r^2 \overset{\text{def}}{=} -k_F$ is different at every r.

The $|k_F|$ decreases all the way to the BB $\implies$ Shells of matter closer to the observer evolve by a Friedmann equation corresponding to larger $|k_F|$.

$\implies$ They are ejected from the BB with larger dS/dt than farther shells, and so intersect the observer's past light cone with a larger velocity than in a model with constant k_F.

$\implies$ Accelerated expansion is imitated – again without introducing "dark energy".

6 A brief conclusion

The theory of relativity has much more to offer to cosmology than the simplistic R–W models found 90 years ago.

Relativistic cosmology made a lot of progress since then.

The inhomogeneous models allow us to explain many of the observed phenomena without introducing any "new physics".

References

[1] G. Lemaître, *Ann. Soc. Sci. Bruxelles* **A53**, 51 (1933); English translation with historical comments: *Gen. Rel. Grav.* **29**, 637 (1997).

[2] R. C. Tolman, *Proc. Nat. Acad. Sci. USA* **20**, 169 (1934); Reprinted with historical comments: *Gen. Rel. Grav.* **29**, 931 (1997).

[3] P. Szekeres, *Commun. Math. Phys.* **41**, 55 (1975).

[4] A. Krasiński, C. Hellaby, *Phys. Rev.* **D65**, 023501 (2002).

[5] A. Krasiński, C. Hellaby, *Phys. Rev.* **D69**, 023502, (2004).

[6] A. Krasiński, C. Hellaby, *Phys. Rev.* **D69**, 043502, (2004).

[7] K. Bolejko, A. Krasiński, C. Hellaby, *Mon. Not. R. Astron. Soc.* **362**, 213, (2005).

[8] A. Krasiński and K. Bolejko, *Phys. Rev.* **D83**, 083503 (2011).

[9] C. Quercellini, M. Quartin and L. Amendola, *Phys.Rev.Lett.* **102**, 151302 (2009).

[10] C. Quercellini, L. Amendola, A. Balbi, P. Cabella, M. Quartin, *Phys. Reports.* **521**, 95 – 134 (2012).

[11] Planck collaboration, *Planck* 2013 results. XVI. Cosmological parameters. arXiv 1303.5076; accepted for *Astronomy and Astrophysics*

[12] H. Iguchi, T. Nakamura and K. Nakao, *Progr. Theor. Phys.* **108**, 809 (2002).

[13] C.-M. Yoo, T. Kai, K-i. Nakao, *Phys. Rev.* **D83**, 043527 (2011).

[14] A. Krasiński, *Phys. Rev.* **D89**, 023520 (2014); erratum: *Phys. Rev.* **D89**, 089901(E) (2014).

[15] A. Krasiński, arXiv:1405.6066, accepted for *Phys. Rev.* **D**.